Published in final edited form as:
Brain Res. 2010 February 8; 1313: 172–184. doi:10.1016/j.brainres.2009.12.006.

Feature Selection in the Human Brain: Electrophysiological Correlates of Sensory Enhancement and Feature Integration

Andreas Keil[1] and **Matthias M. Müller**[2]

[1]University of Florida, Gainesville, FL, USA

[2]University of Leipzig, Leipzig, Germany

Abstract

This study examined the latency and amplitude of cortical processes associated with feature-based visual selective attention, using frequency-domain and time-domain measures derived from dense-array electroencephalography. Participants were asked to identify targets based on conjunctions of three types of object features (color, size, completeness). This procedure aimed to examine (1) the modulation of sensory responses to one or more stimulus features characterizing an object and (2) facilitation and reduction effects associated with competing features, attended and unattended, in the same object. The selection negativity, an event-related potential measure of sensory amplification for attended features, showed a parametric increase of amplitude as a function of the number of attended features. Late oscillations in the gamma band range were also smaller for stimuli with one or more non-attended visual features, but were enhanced for stimuli sharing the overall gestalt with the target. The latency of this late gamma modulation was delayed when two target features were combined, compared to one single discriminative feature. Latency analyses also showed that late bursts of induced high-frequency oscillatory activity peaked around 60 ms later than the selection negativity. Oscillatory activity reflected both selective amplification and competition between object features. These results suggest that sensory amplification of selected features is followed by integrative processing in more widespread networks. Oscillatory activity in these networks is reduced by distraction, and is enhanced when attended features can be mapped to specific action.

Keywords

Feature Selection; Attention; Electroencephalography; Oscillatory Activity; Gamma Band

1. Introduction

When behaving in the context of complex visual environments, humans select a small partition of the available information for in-depth processing. This phenomenon is examined in studies of visual selective attention. Particularly when viewing overlapping or multi-element stimulus arrays, it is important to modulate visual processing to enhance the sensitivity to characteristic features of the to-be-attended object, such as color, size, shape, etc., at the expense of competing task-irrelevant features. Such feature-based attention has been studied extensively in human (Nobre et al., 2006) and non-human subjects (Maunsell and Treue, 2006). Animal and computational modeling studies (Hamker, 2005) have suggested that feature-based selective attention is the result of the cooperative activity in

Corresponding author: Andreas Keil, PhD, Department of Psychology and NIMH Center for the Study of Emotion & Attention, University of Florida, campus and US postal mail: PO Box 112766, Gainesville, FL 32611, courier services: 2800 SW Archer Rd, Bldg 772, Gainesville, FL 32608, Phone: (352) 392-2439, FAX: (352) 392-6047, akeil@ufl.edu.

widespread cortical areas, including the ventral visual stream and frontal cortices (Giesbrecht et al., 2003). In humans, recent multi-modal imaging work has indicated that feature-based attention recruits those areas in sensory cortex that contain neurons specifically sensitive to the feature in question; e.g. area V4 is modulated during color selection (Schoenfeld et al., 2007). Previous research exploiting event-related potentials (ERPs) has converged to suggest that one robust correlate of the attentive selection of stimulus features is the so-called selection negativity (SN), which typically has an onset latency between 130 and 180 ms post-stimulus (Anllo-Vento et al., 1998; Hillyard and Munte, 1984). When using blocked designs and multiple competing object features, other authors (Zhang and Luck, 2009) have found modulation by feature-based attention in earlier segments of the ERP, notably the P1 component (around 100 ms post-stimulus). This can be taken as evidence for a selective modulation of neural activity during feed-forward processing though the visual cortex, as predicted by theoretical models of feature selection and integration (Roelfsema, 2006). By contrast, the SN has been taken as an index of feedback-driven amplification of neural activity in feature-selective cortical regions: Both the latency and amplitude of the SN are sensitive to changes in the nature of the to-be-attended features (Anllo-Vento and Hillyard, 1996), their number and discriminability (Smid et al., 1999), as well as to changing task and contextual demands (Schoenfeld et al., 2007). This amount of flexibility has led some researchers to suggest that feature-based attention should be viewed in a more comprehensive framework of biased competition for resources, with the overall timing and amplitude differences depending on the task requirements (Hopf et al., 2005). Similar task-dependency has been observed with measures derived from time-frequency analyses of electrophysiological data, most notably high-frequency oscillatory activity in the so-called gamma band range (Kaiser and Lutzenberger, 2005). This activity has often been interpreted as a re-entrant large-scale signal that underlies integrative feature processing in multiple cortical areas (Keil et al., 1999), which suggests functional overlap with the SN. In line with this notion, electrophysiological work comparing SN and high-frequency oscillatory activity during color selection found similarities in their sensitivity to experimental manipulations (Müller and Keil, 2004).

Neural mass activity in the gamma frequency range has been referred to as gamma band activity (GBA). It can be reliably observed in the scalp-recorded electroencephalogram (EEG, Frund et al., 2007b; Keil et al., 2003) as well as in local field potentials (Fries et al., 2007), although recent research has raised the question whether some aspects of human GBA in the EEG have an oculomotor, rather than cerebral origin (Yuval-Greenberg et al., 2008). Modeling and experimental studies in non-human mammals have suggested that large-scale GBA reflects multiple microscopic processes: (i) synchronization of excitatory neuronal spike trains belonging to widespread cortical networks associated with separate features of a given stimulus, such as location, color, shape, orientation, etc. and (ii) coupling of interneurons mediating the phase signatures of these networks (Fries et al., 2007).

In human EEG recordings, two pronounced GBA amplitude enhancements are typically seen: Early GBA tends to peak around 100 ms after stimulus onset, in frequency ranges between 25 and 50 Hz. It appears to have a stable phase relationship relative to the stimulus across trials and is often referred to as “early evoked GBA” (Herrmann et al., 1999; Sannita et al., 2001). Early GBA has been shown to vary with physical properties of a visual stimulus (Frund et al., 2007a; Martinovic et al., 2008), aspects of attention and expectation (Herrmann et al., 2004), and motivational relevance (Keil et al., 2007). These properties suggest that early evoked GBA reflects aspects of early visual processing, predominantly oscillations in feed-forward connections (Roelfsema, 2006). The second major modulation in the gamma range occurs later and its onset and phase are typically not tightly linked to the onset of the stimulus. This signal is often seen at 30 Hz and above, peaking in time ranges between 200 and 400 ms after stimulus onset, and has been discussed as a neural correlate of

object recognition (Tallon-Baudry and Bertrand, 1999), memory formation and recall (Gruber et al., 2004; Tallon-Baudry et al., 1998), and visual selective attention (Gruber et al., 1999; Womelsdorf and Fries, 2006), among other functions of the human central nervous system (for a review, see Kaiser and Lutzenberger, 2005; Keil et al., 2001a). Here we will focus on this second type of GBA, non-phase-locked to the onset of the stimulus, and appearing around 300 ms post-stimulus.

Given its above-mentioned sensitivity to experimental manipulations of object features and attention selection, the time-varying amplitude of the human GBA is an obvious candidate variable for studying cortical processes associated with the selection and integration of attended features forming a task-relevant, meaningful object. Specifically, it may complement the information contained in the ERP-derived SN amplitude. In a previous study examining the SN and GBA during color selection (Müller and Keil, 2004), we found that both the GBA and the SN were related to attentive stimulus feature processing. Significant differences however were observed in terms of timing and topography. Overall, the top-down attentional processing of color resulted in high-frequency synchronization of neuronal activity in posterior cortical areas, which was reliably observed in time ranges during but also after the SN time window (i.e., 160-280 ms). This pattern of results suggested that feature-based attention involves large-scale increases of neural mass activity in sensory areas along the ventral stream, as indexed by the SN, and multiple parallel, temporally more extended, oscillatory processes potentially reflecting integrative neural processing.

Three questions arise on the basis of these findings: First, what is the relationship between the sensory amplification of multiple selected features and subsequent integrative processing? Second, how is the latency of both responses affected by manipulating the number of attended features and the difficulty of the task? And last, is there evidence for suppression of either response (SN, GBA, or both) when unattended features are present?

In the present study, we addressed these questions by systematically manipulating the object features (color, size, completeness) necessary to identify the target stimulus in a given block of trials. This design allows considering differences in brain activity between conditions requiring integration of zero, one, or two attended features. By virtue of comparing conditions with different numbers and different kinds of target features to be integrated, it is possible to analyze the specific aspect of the brain electric response that is related to selecting a specific feature in an attended object (i.e. comparing objects with all versus all minus one attended features) or non-attended object (i.e., comparing objects with one versus none attended features). In addition to behavioral responses, the selection negativity (SN), a well-established index of selective sensory processing of attended visual features as well as GBA changes were examined as dependent variables. Given the literature outlined above, it was expected that increasing the number of relevant features, attentive selection of features for sensory amplification as indexed by the selection negativity would take longer and recruit more resources, reflected in greater amplitude and longer latency of the SN. In terms of the late GBA amplitude, we hypothesized that attended stimuli (i.e., those with more than one attended feature) should provoke integrative processing and thus show GBA enhancement relative to baseline. In the same vein, the presence of unattended (i.e. distractor) features was expected to be associated with a relative reduction of time-varying power for the late-induced GBA.

2. Results

2.1 Behavioral data

Hits, misses, and false alarms were analyzed separately for target types, identified by 4 possible feature conjunctions (turquoise/small, turquoise/big, green/small, green/big). The hit rate (overall: 91.2 percent, SD = 3.8 percent) and response time (overall: 396 ms, SD = 64 ms) did not vary as a function of target type ($F(3, 36) = .98$, n.s.), but false alarms were more frequent for standards of the same color as the target (false alarm rate = 4.1 percent, SD = 1.8 percent) than for the standards having the same size as the target (false alarm rate = 1.1 percent, SD = 0.5 percent), $t(12) = 3.2$, $p < .05$.

2.2 Method check: P300 amplitude

Paralleling behavioral results, no main effect or interaction involving the feature conjunction conditions were found (Fs < 2, n. s.). By contrast, P300 amplitude in the target conditions was significantly greater across feature conjunction conditions, $F(1,12) = 60.4$, $p < .001$, than P300 to attended standards (i.e., the same stimulus as the respective target, but with no check missing), which supports the notion that participants were compliant and that feature conjunctions did not differ in difficulty or saliency (see supplementary Figure 2).

2.3 Event-Related Potentials: Amplitude of the Selection Negativity

ERP waveforms showed parametric sensitivity to the experimental conditions, beginning after the peak of the N1 component, at around 190 ms post-stimulus (see Figure 2). Omnibus ANOVA comparing the amplitude in the SN time window (180-330 ms) across all 4 conditions showed main effects of attended color, suggesting more negativity for attended than for the unattended color across the scalp, $F(1,12) = 28.3$, $p < .001$. The attended size of the checkerboards was likewise related to greater negativity than the unattended size, across scalp locations, $F(1,12) = 24.1$, $p < .001$. Attention to color and size interacted, with attention to size affecting the SN more in attended color trials than in non-attended color trials, $F(1,12) = 11.1$, $p < .001$. We followed these overall effects using post-hoc ANOVAs for each feature by attention combination to specifically assess the presence of effects of attention to one feature as a function of attention to the other feature.

Size selection with target color present ([S+C+]-[S-C+])—Perceiving the attended size was associated with greater negativity, compared to the non-target size, when the stimulus at the same time contained the target color stimulus: main effect of attention, $F(1,12) = 27.9$, $p < .001$. This difference between the attended and unattended size was more pronounced at posterior sites, which led to an interaction of attention and location, $F(1,12) = 26.5$, $p < .001$, see Figures 3 and 4. When followed up using corrected t-tests, the greater negativity for the attended size was seen at electrodes Po7, Po8, O1, and O2, $ts(12)_{corrected} > 2.9$.

Color selection with target size present ([S+C+]-[S+C-])—A similar pattern emerged for the color selection. A main effect of attention indicated that negativity was greater for the attended versus the non-attended color across electrode sites, $F(1,12) = 30.0$, $p < .001$. Again, this pattern was more pronounced at posterior electrodes (P7, P3, O2, Po8), attention X location, $F(1,12) = 43.6$, $p < .001$.

Size selection with target color absent ([S+C-]-[S-C-])—Effects of size selection were small and focal when the stimulus was drawn in the unattended color. We observed a four way interaction of attention, hemisphere, location, and electrode, $F(5,60) = 3.9$, $p < .05$. When this interaction was further examined with t-tests, attention effects were found at right parietal and bi-lateral frontal sensors only, suggesting greater negativity for attended than

unattended size at posterior electrodes Po8, P4, P8, $ts(12)_{corrected} > 2.9$, and greater positivity at frontal sites F8 and F3, $ts(12)_{corrected} > 2.5$.

Color selection with target size absent ([S-C+]-[S-C-])—Absence of a second attended feature also attenuated the effects of color selection, but to a lesser degree than for the size selection condition described above. As indicated by an attention X location interaction, $F(1,12) = 5.7$, $p < .05$, negativity for the attended color was greater than for the unattended color at posterior sites.

2.4 Event-Related Potentials: Latency of the Selection Negativity

Differences in SN latency between the attention conditions were evaluated using jackknifed t-tests (see methods) for the waveforms recorded at sensors O1 and O2, where the SN was most pronounced. In particular, the hypothesis was tested that attending to more features (i.e. selection with target size/color present) would be related to longer SN latency compared to selection of only one feature (no other target feature present). In addition, we compared size and color selection in terms of latency.

Selection of one feature (no other target feature present, respectively) tended to be faster than selection of two features on the left hemisphere, $t_{jackknife}(1,12) = 2.1$, $p = .06$, with the mean difference being 36 ms. The same difference reached significance on the right hemisphere, $t_{jackknife}(1,12) = 3.9$, $p < .01$, with the SN associated with the selection of a single feature leading the two-feature SN by 49 ms. Evidence for a faster selection of color features in general was seen on the right hemisphere (i.e. at site O2), with the SN for color selection leading the size selection SN by 31 ms, $t_{jackknife}(1,12) = 2.7$, $p < .05$. No difference was observed on the left hemisphere (see Figure 3, left).

2.5 Gamma Band Changes: High Induced Gamma

Differences in spectral changes were evaluated according to the same logic as ERPs, with baseline-corrected spectral power as the dependent variable. An additional focus was on examining anterior effects, which may contribute to the GBA modulations as measured over posterior sensors. Grand mean time-frequency representations of the four conditions of interest are shown in Figure 5.

In contrast to ERP measures, omnibus ANOVA for induced GBA showed no main effects of attention across scalp regions. By contrast, GBA activity was sensitive to the interaction of attended size and attended color, specifically at posterior sites: Attended size X attended color X location, $F(1,12) = 9.2$, $p < .01$. Again, this interaction terms was followed up using ANOVAs assess the presence of effects of attention to one feature as a function of attention to the other feature.

Size selection with target color present ([S+C+]-[S-C+])—Amplitude increase was observed as a function of size selection specifically at right posterior, $t(12)_{corrected} = 3.5$, $p < .01$, and right anterior sites, $t(12)_{corrected} = 2.8$, $p < .05$, whereas no difference was found at left posterior and left anterior regions, $F(1, 12) = 6.0$, $p < .05$. No further effect reached significance (see Figure 6, top left).

Color selection with target size present ([S+C+]-[S+C-])—Paralleling ERP results, attention effects were somewhat more pronounced for the color selection, resulting in an interaction between attention and location, $F(1, 12) = 5.0$, $p < .05$. Thus, across hemispheres, posterior spectral power was greater for attended than non-attended stimuli (see Figure 6, top right). Again, other effects did not reach significance.

Size selection with target color absent ([S+C-]-[S-C-])—As opposed to ERP results as well as results with the second feature being the attended one (above), size selection of stimuli having non-attended color as a second feature resulted in pronounced posterior decrease of gamma-band spectral changes, attention X location, $F(1,12) = 5.2$, $p < .05$. This effect was present across hemispheres and was not observed at anterior electrodes.

Color selection with target size absent ([S-C+]-[S-C-])—A tendency in the same direction was observed for color selection with non-attended size present, $F(1,12) = 2.8$, n.s., but neither this difference nor any other effect reached significance. Importantly, no evidence was observed indicating increase of the oscillatory response in this condition.

2.6 Latency of induced gamma versus the selection negativity

Latencies across measures were compared for time series representing regional averages, for maximum signal-to-noise, i.e. the SN was averaged across O1 and O2 and the induced GBA waveform was extracted from the posterior sites used for creation of time-frequency plots, i.e., P3/P4, P7/P8, P03/PO4, P07/P08, 01/02, and P9/P10. Because SN and GBA attention differences were reliable in the conditions with an additional target feature present (i.e. selection of two features), only these conditions were included for latency analysis. The resulting time series are shown in Figure 7 together with vertical bars indicating the mean time point when each waveform reached the 50% amplitude criterion (see methods) and the jackknifed standard error of the difference (gray box). As illustrated in the figure, the selection negativity led the GBA difference by 58 ms, with a standard error of 21 ms, resulting in a significant latency difference between the two measures, $t_{jackknife}(1,12) = 2.7$, $p < .05$.

3. Discussion

There is an ongoing debate as to the functional role of large-scale oscillatory brain activity for human perception and attentive processing. The present study examined latency and amplitude of brain processes associated with feature-based visual selective attention, using frequency-domain and time-frequency-domain measures derived from dense-array electroencephalography. Manipulating the number of these object features necessary to uniquely identify the target stimulus, we aimed to examine (a) the processes of sensory enhancement of selected features relative to different numbers and types of competing features, and (b) the attentive integration of selected features in attended versus unattended visual objects. Our overarching hypothesis was that the two processes would show differential sensitivity to the experimental manipulation, with (1) linear variations of SN amplitude reflecting sensory selection of varying numbers of features and (2) GBA enhancement solely in the “attended” conditions, showing relative power reduction when objects contain unattended features. In particular, late induced GBA was considered in the context of attentive feature integration and action preparation.

The main results of the study showed the expected pattern of amplitude enhancement of the SN, taken to reflect increasing sensory enhancement as the number of attended features increased. Enhancement of induced GBA as a function of selective attention was observed when stimuli contained at least two out of three attended features. Thus, stimuli sharing the overall configuration with the target (i.e., color and size) induced greater GBA than stimuli having less overlap with the target stimulus. With the overall amount of attention to the object reduced (i.e., only one out of three target features present), late induced GBA showed reduced power also, being significantly smaller in trials with one target feature than in trials without any target features. In the following, we discuss the implications of these main results vis-à-vis the hypotheses.

3.1 Parametric variation of the SN: amplitude and latency

Replicating a host of previous studies, we found that the attentive selection of stimulus features resulted in a parametric increase of SN amplitude as a function of the number of selected features (Anllo-Vento et al., 1998). Earlier work has studied how conjunctions of multiple stimulus features are reflected in ERP differences and has found that particularly the early segment of the SN additively reflects the number of features necessary to perform a selection task (Smid et al., 1999). This notion is consistent with hemodynamic imaging data that support area-specific modulation of the evoked sensory response in those cortical regions that are sensitive to a particular feature such as color or motion (McMains et al., 2007). In our study, selection of features lasted longer when two features needed to be processed, compared to one single discriminant feature, as indicated by jackknife-base latency analyses of the SN across conditions. This result can be predicted based on behavioral data indicating that temporal resolution of feature perception declines as a function of the number of to-be-attended features (Bodelon et al., 2007). When comparing latencies of oscillatory activity and the SN, we observed that the induced GBA attention difference reached significance 60 ms later than the selection negativity. Together with the differential sensitivity to the experimental manipulations as described above, this temporal pattern is suggestive of a higher-order integrative process, reflected by high-frequency oscillations. In an earlier study of SN and GBA, participants selected for color only and were not presented with conjunction processing of more than one feature (Müller and Keil, 2004). In this earlier research, we demonstrated that the high-induced GBA peaked at the same latency as the SN did, but extended into the same time range as in the present study, i.e. between 250 and 380 ms after stimulus onset. In a similar manner, SN peaked earlier (around 200 ms) in the single-feature task, compared to the current multi-feature task, which showed a peak latency of 280 ms. Taken together, the present ERP data show that stimulus-selective neural masses are amplified in a time-locked manner, facilitating the perceptual processing of relevant features. Earlier reports have speculated whether the integration of features, or conjunction processing, may impact the later segment of the SN, or subsequent components of the ERP (Smid et al., 1999). In the present study, we also examined the sensitivity of late induced gamma oscillations to the experimental manipulations, to determine their potential role in feature selection.

3.2 GBA enhancement for relevant and reduction for irrelevant attended features

As in previous studies, induced GBA was observed in a time range between 250 and 380 ms after stimulus onset. Late induced GBA displayed a qualitatively different pattern of results compared to the SN data. Most notably, we found pronounced posterior enhancement of the induced GBA solely for conditions that shared two features with the target (i.e. color and size). Significant relative reduction of GBA was seen when there was only one attended feature, compared to the condition with no attended feature. Overall, this is in line with an interpretation of configural processing of targets and target-like stimuli in the oscillatory networks involved in integration of selected features, potentially involving synchronization in a network that encompasses higher-order visual representations, but also response representations (Keil et al., 2007; Singer et al., 1997). Such a notion would predict stronger suppression for non-target stimuli containing salient target features, thus acting as powerful distractors. As an alternative explanation, response inhibition processes may be considered (e.g. Keil et al., 2001b). Such an account would predict, however, that inhibition of a motor response is greatest for attended standards, and smallest for non-attended standards (i.e., stimuli containing no target feature). By contrast, the present pattern of results suggests that GBA varies to be enhanced for attended features, suppressed when distracting features are present, and slightly above baseline for a non-attended stimulus. In the animal model, higher-order cortical areas (i.e., area V4 in Macaque Monkeys) were recently associated with mapping of selected features onto response representations (Mirabella et al., 2007),

which contributed to the control of task-dependent behavior. The topography and timing of the GBA modulations observed in the current study make the GBA a candidate mechanism that may underlie such integrative neural computation, linking attended perceptual features to action.

3.3 Methodological concerns

When measuring small signals in the human EEG, it is mandatory to ensure that the signals reflect cranial rather than artifactual activity in the frequency range of interest. With respect to GBA, there have been debates about their validity and potential origin since the first reports of GBA modulation by cognitive tasks in human participants (Kristeva-Feige et al., 1993; Tallon et al., 1995). Criticisms included that high-frequency oscillation may be harmonics of alpha modulation (Jürgens et al., 1995), which was rejected because alpha and gamma often show uncorrelated sensitivity to experimental manipulations (Keil et al., 2001b; Lutzenberger et al., 1997). Recently, Yuval-Greenberg and colleagues published an intriguing study in which they showed that micro-saccades in response to visual stimuli may elicit sharp voltage peaks that are oculomuscular in origin, but may appear as high-frequency oscillations at posterior electrodes around 200-400 ms after stimulus onset (Yuval-Greenberg et al., 2008). Based on their results, they concluded that transient GBA recorded by scalp EEG might often reflect miniature saccade dynamics, rather than neuronal oscillations. In the present study, this is a concern because the stimuli were extending into parafoveal regions of the visual field, and thus might have triggered saccade activity, as participants worked on the detection of missing checks. One strong prediction of Yuval-Greenberg and colleagues is that saccade-related activity should be clearly visible at ocular electrodes, when using the average reference. In the present study, we used the average reference throughout and explicitly conducted the same statistical tests as performed for the overall electrode set on each peri-ocular sensor. This procedure should be an index of any ocular contribution to differences found over posterior regions. We did not use a source estimation algorithm that might obscure the putative contribution of saccade-related oscillatory activity. Using the present statistical approach, which aimed to maximize sensitivity to putative saccade-related high-frequency phenomena, we did not find any evidence for systematic GBA modulation around the areas of the eyes that would follow the experimental differences found at posterior sensors.

3.4 Conclusions and future directions

Taken together, the present results are in line with a host of human and animal studies, converging to demonstrate enhanced high-frequency neural oscillations in response to attended visual cues. They suggest that neural amplification and integrative processing of selected features, although highly parallel processes, may be reflected in two overlapping correlates in the human EEG, one being primarily time-locked and the other being visible in induced (non-time-locked) high-frequency oscillations. The duration of sensory amplification of attended features and subsequent integrative feature processing varies as a function of the number of features necessary to uniquely identify a target or non-target stimulus. What remains unclear is the relationship between functional and structural specificity as observed for the SN previously (McMains et al., 2007) and the neuroanatomical location of GBA modulations. This is essential to understand the functional role of GBA in the context of feature selection and integration. Future work may employ multimodal imaging approaches to study these oscillatory processes with greater spatial accuracy.

4. Experimental Procedure

4.1 Subjects

Thirteen right-handed students (5 males) with normal or corrected-to-normal vision participated in the study. Based on the effect sizes observed in a previous study (Müller and Keil, 2004), we found that a sample size of 12 or more would be needed to detect reliable condition-related differences in SN and GBA. Their mean age was 24.6 years (range: 20 – 31 years). Written informed consent was obtained from each subject after the nature of the study was fully explained. Approval was obtained from the internal review board.

4.2 Stimuli and task

Stimuli were green-and-gray and turquoise-and-gray checkerboards varying with respect to three feature dimensions (color, check size, and completeness; see below). Checkerboards were presented foveally for 200 ms on the center of a 21-inch monitor, situated 1.5 m in front of the subjects, replicating the setup of an earlier study in our laboratory (Müller and Keil, 2004). From this viewing distance the checkerboards subtended 4.0 deg. × 4.0 deg. of visual angle. The center check contained a fixation cross, which was present throughout the experiment. For all checkerboards, target stimuli ($p = 0.20$) were designed by omitting one colored check at a random position, respectively (see Figure 1). Using an omission as a the target feature, it was ensured that the attended standard (non-target) stimuli shared two features (color, size) with the target in a given block, but did not contain a salient non-target feature on a different feature dimension (brightness, shape), which could lead to interference and suppression.

Target and non-target checkerboards were presented in randomized order, with an inter-stimulus-interval randomly varying between 1000 and 1500 ms in 8 blocks of 182 trials each. Duration of one block was approximately 9 minutes. At the beginning of each block, subjects were instructed to manually respond to the target stimulus, which was marked by one missing check and one out of four distinct feature combinations: (a) green/big checks; (b) green/small checks; (c) turquoise/big checks; (d) turquoise/small checks. Big checks resulted in four by four checkerboards, with each check covering four times the area of the small checks, which were shown as 8 by 8 checkerboards. As a consequence, the overall colored area and luminance was equal between big and small block checkerboards. Luminance for non-target stimuli was 16.9 cd/sqm. Participants were asked to only press the space bar of the computer keyboard when they detected a target, and to do so as fast and as accurately as possible. The target combination of features was designated block-wise in counter-balanced order. Furthermore, the responding hand was changed halfway through the experiment, and the sequence of hand usage was counterbalanced across subjects. Subjects were also instructed to avoid blinks and eye-movements and to maintain gaze onto the central fixation cross. Practice trials were provided for each subject for each condition to make sure that every subject fully understood the task.

4.3 Electrophysiological recordings

EEG was recorded continuously with an EGI (Electrical Geodesics) 129-electrode array. A schematic representation of the electrode array and corresponding extended international 10-20 electrode sites is given in supplementary Figure 1. The vertex (recording site Cz) was used as the reference during recording. As suggested for the EGI high input impedance amplifier, impedance was kept below 50 kOhms for each electrode. Sampling rate was 500 Hz and all channels were preprocessed on-line by means of a 0.1 to 200 Hz band-pass filter. In addition, vertical and horizontal eye movements were monitored with a subset of the 129 electrodes. Further data processing was performed off-line.

4.4 Data analysis

Behavioral data—Only reaction times between 150 and 1500 ms after target onset were considered to be correct responses. Reaction times shorter or longer than that period were considered as missed responses. Hits, misses, and false alarms were analyzed separately for target types, identified by 4 possible feature conjunctions (turquoise/small, turquoise/big, green/small, green/big). Differences among these conditions were evaluated by means of analysis of variance (ANOVA) with a 4-level factor of Condition (see above, total of 4 conjunction types), and followed up by t-tests corrected with the Bonferroni-Dunn method.

Epochs and rejection of trials—Only non-target stimuli were included in the main analyses. Target trials were analyzed in a separate manipulation check (see below), in which P3 amplitude was evaluated. This was (a) in order to exclude possible interference with the motor response, (b) because targets occurred only in 20 % of the trials, resulting in a substantially lower signal-to-noise ratio as compared to non-targets, and (c) because of the systematic brightness difference associated with the omitted check. For further analysis, single epochs of 1024 ms length (300 ms before and 724 ms after stimulus onset) were extracted. These epochs were submitted for artifact rejection and correction using a procedure developed by Junghöfer and co-wokers (Junghöfer et al., 2000). This procedure uses a combination of trial exclusion and channel approximation based on statistical parameters of the data. In a first step, artifacts are detected using the recording reference (Cz). Subsequently, global artifacts are detected using the average reference. In a next interactive step, distinct sensors from particular trials are removed on the basis of the distribution of their amplitude, standard deviation and gradient. The information of eliminated electrodes is replaced with a statistically weighted spherical interpolation from the full channel set. In a last step, the variance of the signal across trials is computed to document the stability of the average waveform. The limit for the number of approximated channels was set to 20 channels. With respect to the spatial arrangement of the approximated sensors, it was ensured that the rejected sensors were not located within one region of the scalp. Single epochs with excessive eye-movements and blinks or more than 20 channels containing artifacts were discarded. The remaining data were stored and were then further inspected for potential small ocular artifacts: Horizontal and vertical EOG time series were generated by re-referencing of peri-ocular channels 125 and 128 as well as 126 and 14, respectively to bi-polar montages. Trials with remaining ocular artifacts (movement exceeding 50 μV and all blinks) were rejected. For the 13 subjects in our sample, the average rejection rate with this very conservative threshold was 31 % for non-target stimuli and 32 % for target stimuli (valid target epochs were used for a method check analysis of the P300 component of the ERP). Across participants, the percentage of acceptable trials ranged from 59.5 to 89 percent. For all subsequent analyses, the average reference was used.

Trial averaging and experimental conditions—Four ERPs reflecting the four attention conditions were formed by averaging across non-target trials for all possible feature combinations, after making sure that each combination contributed similar amounts of experimental trials to each attention condition: green/big checks: 71% good trials; green/small checks: 69%; turquoise/big checks: 70%; turquoise/small checks: 74%. When tested statistically using uncorrected t-tests, for high sensitivity to potential differences, none of the tests approached significance (all $ts < 1.6$). This is important in the light of recent reports suggesting that spatial frequency may systematically affect measures of oscillatory activity (Frund et al., 2007a). Hence, four different averages for the electrophysiological dependent variables (ERP, time-varying spectral power) were obtained reflecting that (i) the stimulus had the target size and target color (S+C+), (ii) the stimulus had the target size but not target color (S+C-), (iii) the stimulus did not have the target size, but had the target color (S-C+), and (iv) the stimulus had neither the target size nor target color (S-C-). Mean reaction time

and percentage of correctly detected targets were determined for target conditions across colors and sizes and were subjected to ANOVA and paired t-tests as described above.

Event-related potentials—Each ERP was calculated as change relative to the mean pre-stimulus amplitude. All incomplete (missing one check) stimuli were excluded from these analyses. In order to extract the SN, attentional difference waves were obtained by subtracting the ERP according the four attention conditions described above (Anllo-Vento et al., 1998; Hillyard and Anllo-Vento, 1998). We focused on four differences reflecting (i) size selection with target color present *([S+C+]-[S-C+])*, (ii) color selection with target size present *([S+C+]-[S+C-])*, (iii) size selection with target color absent *([S+C-]-[S-C-])*, and (iv) color selection with target size absent *([S-C+]-[S-C-])*. The time window for the SN was selected (a) based on a previous study in the same laboratory and same equipment, (b) previous feature-based attention work (e.g. Schoenfeld et al., 2007), and (c) the grand mean difference waves across all subjects (see Figure 3). These three criteria converged and suggested extraction of a mean amplitude in the time segment between 180 and 330 ms post-stimulus that reliably represented the selection negativity. In addition, we extracted the P300 ERP component in response to target stimuli to obtain an objective physiological measure for participants' compliance: amplitudes for target and non-target trials were averaged separately, and a mean across parietal electrodes sites corresponding to the sites Pz and POz of the international 10-20 system and their nearest neighbors (see below) was formed in a time window extending between 380 and 480 ms post-stimulus.

Spectral analysis—Oscillatory activity was analyzed according to the standard procedure employed in a number of preceding studies (e.g., Gruber et al., 2004; Keil et al., 2003). In brief, spectral changes in oscillatory activity were analyzed by means of Morlet wavelet analysis (Bertrand et al., 1994), which provides a good compromise between time and frequency resolution (Tallon-Baudry and Bertrand, 1999). This method yields a time-varying magnitude of the signal in each frequency band leading to a time-by-frequency (TF) representation of the signal and is described in-depth, together with suggested parameter definitions in Tallon-Baudry and Bertrand (1999). In order to achieve good time and frequency resolution in the gamma frequency range the wavelet family was defined by a constant $m = f_0/\text{sigma}(f) = 7$, with the center frequency f_0 ranging from 9.77 to 79.84 Hz in 0.49 Hz steps. Sigma(f) is the width of the wavelet in the frequency domain (full-with at half maximum, FWHM). This resulted in a time resolution of ± 26 ms (FWHM) at a frequency of 40 Hz, which marked the lower border of the frequency range selected to index induced GBA (see below).

Analysis of total GBA: Time-varying energy in a given frequency band was calculated for each recording epoch as the squared absolute value of the convolution of the signal with the wavelet for each complex spectrum. An epoch from 280 to 100 ms prior to stimulus onset was used as an estimate of general noise. The mean of this baseline epoch was subtracted from TF matrices for each frequency and time point for each electrode, respectively. For graphical illustration, values were then expressed as change with respect to the mean of the baseline.

In order to estimate the frequency and time ranges for statistical analysis of oscillatory activity, all evolutionary spectra were averaged across all posterior electrode sites (corresponding 10-20 positions: CP1/2, P7/8, P3/4, PO7/8, PO3/4, O1/2, Pz, and POz; see supplementary figure 1) and the four attention conditions as described above. These electrode sites were selected on the basis of previous studies of visual information processing (e.g., Gruber et al., 2004). Based on these steps, we identified a reliable enhancement of spectral power in the expected time-frequency range, for each individual and condition. This high-frequency oscillatory response occurred around 300 ms in time,

and is typically referred to as “induced GBA”, because it is typically not time- and phase-locked to the stimulus onset. Accordingly, in the present study, no significant phase-locking values were seen in the induced GBA range in any of the participants and experimental conditions. The induced GBA was scored as the mean spectral change between 250 and 380 ms post-stimulus, in a frequency range between 40 and 78 Hz.

Difference spectra were then obtained and grand mean differences between conditions were plotted for illustration purposes, in the same manner as for the ERP difference waves. Electrode sites used for these TF-plots were selected on the basis of previous GBA studies on visual information processing (e.g., Gruber et al., 2004, Keil et al., 2003). Identical to the procedure for obtaining the SN, the grand mean posterior evolutionary spectrum of unattended non-targets was subtracted from the grand mean posterior evolutionary spectrum across all attended non-targets to identify the latency and frequency range of gamma power peaks of interest (see Results).

Topographical distribution of voltage and spectral power—All topographies reflect spline interpolations of the data collected at 129 electrodes, mapped to the surface of the scalp using the method suggested by Junghöfer and colleagues (Junghöfer et al., 1997). To that end, we used the open source toolbox EMEGS, a collection of Matlab functions that allows analysis of EEG/MEG data provided by Peter Peyk and Markus Junghöfer (see http://134.34.43.26/~emegs/modules/news/).

Statistical Analysis—For all statistical analyses, we used a subset of electrodes that covered all regions of the scalp, to ensure sensitivity to electrocortical processes over posterior, but also anterior regions, which is pivotal to study the topographical specificity of the differences observed. Paralleling an earlier study (Müller and Keil, 2004), we selected 24 electrodes placed at modified 10-20 electrode sites (American Electroencephalographic Society, 1991): F7/F8, F3/F4, C3/C4, T7/T8, CP5/CP6, CP1/CP2, P3/P4, P7/P8, P03/PO4, P07/P08, 01/02, and P9/P10. The locations of these sites are indicated schematically in supplementary Figure 1.

In a first step, overall effects of experimental manipulations across all conditions were evaluated by means of omnibus repeated-measures ANOVAs with factors of attended size (attended vs. ignored), attended color (attended vs. ignored), location (anterior vs. posterior sites), hemisphere (left, right), and site (6 sites in each quadrant, see above). In a subsequent step, aiming to follow up interactions emerging in this overall ANOVA, we evaluated attentional selection effects for one feature in the presence of the respective other feature (e.g., S+C+ versus S-C+: size selection with target color present) as well as in the absence of the other target feature (e.g. S-C+ versus S-C-: color selection with target size absent), for all dependent variables (ERP and spectral measures) and each discriminative feature (size and color) separately: Amplitude differences between these pairs of conditions were evaluated by means of repeated-measures ANOVAs with factors of attention (attended vs. ignored target), location (anterior vs. posterior sites), hemisphere (left, right), and site (6 sites in each quadrant, see above). This design allows to analyze groups of EEG sensors, but also to follow up these single sensors within a specific area by means of post-hoc tests, enhancing spatial specificity.

The P300 was examined by extracting the mean baseline corrected amplitude for electrode locations CP1/2, PO3/4, P3/4, and Pz, since the P300 typically exhibits maximum amplitude at parietal electrodes (Polich and Kok, 1995). P300 amplitude differences were then evaluated by means of repeated-measures ANOVA with factors of targetness (target versus non-target) and feature conjunction type (green/big checks; green/small checks; turquoise/big checks; turquoise/small checks).

Analysis of Latency Differences—Latency differences were evaluated by means of t-tests for selected electrodes showing reliable amplitude effects, using the jackknife method (Kiesel et al., 2008). This method was selected because it has been shown to be more sensitive to real latency differences than single-subject-based scoring methods while at the same time being less affected by noise. Because Jackknife-based statistics involve re-computation of the desired test statistic, leaving out one observation at a time from the sample set. In the present case, 13 new averaged waveforms were formed to replace each of the 13 participants' individual waveforms/time varying spectra for each condition. Each of these waveforms/time-varying spectra represented a grand mean across all participants but one. Leaving out each participant in one of the averages thus led to 13 new averages, from which the dependent variables were extracted. The latency of each event of interest (selection negativity, late GBA) was scored as the point in time when 50% of the maximum amplitude of that event was reached. Thus, latency differences between events were determined for the grand mean and for the 13 new dependent variables. Jackknife t-values were then calculated as the ratio of the grand mean difference in ms, divided by the jackknife estimate of the standard error of the difference sD, as described in Miller et al. (1998).

The same approach was used to examine latency differences between GBA and ERP derived measures. All reported p-values were adjusted by the Huynh-Feldt-epsilon procedure where necessary. Post-hoc tests were carried out using paired t-tests adjusted by the Bonferroni-Dunn criterion. Means and standard errors are presented throughout the paper.

Supplementary Material

Refer to Web version on PubMed Central for supplementary material.

Acknowledgments

This work was supported by the Deutsche Forschungsgemeinschaft and by a grant from the Kurt Lion foundation to AK. The authors would like to thank Gundula Graessle for help in data collection.

References

Anllo-Vento L, Hillyard SA. Selective attention to the color and direction of moving stimuli: electrophysiological correlates of hierarchical feature selection. Percept Psychophys. 1996; 58:191–206. [PubMed: 8838164]

Anllo-Vento L, Luck SJ, Hillyard SA. Spatio-temporal dynamics of attention to color: evidence from human electrophysiology. Hum Brain Mapp. 1998; 6:216–38. [PubMed: 9704262]

Bertrand O, Bohorquez J, Pernier J. Time-frequency digital filtering based on an invertible wavelet transform: an application to evoked potentials. IEEE Trans Biomed Eng. 1994; 41:77–88. [PubMed: 8200671]

Bodelon C, Fallah M, Reynolds JH. Temporal resolution for the perception of features and conjunctions. J Neurosci. 2007; 27:725–30. [PubMed: 17251411]

Fries P, Nikolic D, Singer W. The gamma cycle. Trends Neurosci. 2007; 30:309–16. [PubMed: 17555828]

Frund I, Busch NA, Korner U, Schadow J, Herrmann CS. EEG oscillations in the gamma and alpha range respond differently to spatial frequency. Vision Res. 2007a; 47:2086–98. [PubMed: 17562345]

Frund I, Schadow J, Busch NA, Korner U, Herrmann CS. Evoked gamma oscillations in human scalp EEG are test-retest reliable. Clin Neurophysiol. 2007b; 118:221–7. [PubMed: 17126070]

Giesbrecht B, Woldorff MG, Song AW, Mangun GR. Neural mechanisms of top-down control during spatial and feature attention. Neuroimage. 2003; 19:496–512. [PubMed: 12880783]

Gruber T, Müller MM, Keil A, Elbert T. Selective visual-spatial attention alters induced gamma band responses in the human EEG. Clinical Neurophysiology. 1999; 110:2074–2085. [PubMed: 10616112]

Gruber T, Tsivilis D, Montaldi D, Muller MM. Induced gamma band responses: an early marker of memory encoding and retrieval. Neuroreport. 2004; 15:1837–41. [PubMed: 15257158]

Hamker FH. The reentry hypothesis: the putative interaction of the frontal eye field, ventrolateral prefrontal cortex, and areas V4, IT for attention and eye movement. Cereb Cortex. 2005; 15:431–47. [PubMed: 15749987]

Herrmann CS, Mecklinger A, Pfeifer E. Gamma responses and ERPs in a visual classification task. Clin Neurophysiol. 1999; 110:636–42. [PubMed: 10378732]

Herrmann CS, Munk MH, Engel AK. Cognitive functions of gamma-band activity: memory match and utilization. Trends Cogn Sci. 2004; 8:347–55. [PubMed: 15335461]

Hillyard SA, Munte TF. Selective attention to color and location: an analysis with event-related brain potentials. Percept Psychophys. 1984; 36:185–98. [PubMed: 6514528]

Hillyard SA, Anllo-Vento L. Event-related brain potentials in the study of visual selective attention. Proc Natl Acad Sci U S A. 1998; 95:781–7. [PubMed: 9448241]

Hopf JM, Schoenfeld MA, Heinze HJ. The temporal flexibility of attentional selection in the visual cortex. Curr Opin Neurobiol. 2005; 15:183–7. [PubMed: 15831400]

Junghöfer M, Elbert T, Leiderer P, Berg P, Rockstroh B. Mapping EEG-potentials on the surface of the brain: a strategy for uncovering cortical sources. Brain Topogr. 1997; 9:203–17. [PubMed: 9104831]

Junghöfer M, Elbert T, Tucker DM, Rockstroh B. Statistical control of artifacts in dense array EEG/MEG studies. Psychophysiology. 2000; 37:523–32. [PubMed: 10934911]

Jürgens E, Rosler F, Henninghausen E, Heil M. Stimulus-induced gamma oscillations: harmonics of alpha activity? Neuroreport. 1995; 6:813–6. [PubMed: 7605953]

Kaiser J, Lutzenberger W. Human gamma-band activity: a window to cognitive processing. Neuroreport. 2005; 16:207–11. [PubMed: 15706221]

Keil A, Muller MM, Ray WJ, Gruber T, Elbert Ts. Human gamma band activity and perception of a gestalt. J Neurosci. 1999; 19:7152–7161. [PubMed: 10436068]

Keil A, Gruber T, Muller MM. Functional correlates of macroscopic high-frequency brain activity in the human visual system. Neurosci Biobehav Rev. 2001a; 25:527–34. [PubMed: 11595272]

Keil A, Muller MM, Gruber T, Wienbruch C, Elbert T. Human large-scale oscillatory brain activity during an operant shaping procedure. Brain Res Cogn Brain Res. 2001b; 12:397–407. [PubMed: 11689299]

Keil A, Stolarova M, Heim S, Gruber T, Muller MM. Temporal stability of high-frequency brain oscillations in the human EEG. Brain Topogr. 2003; 16:101–10. [PubMed: 14977203]

Keil A, Stolarova M, Moratti S, Ray WJ. Adaptation in visual cortex as a mechanism for rapid discrimination of aversive stimuli. Neuroimage. 2007; 36:472–479. [PubMed: 17451974]

Kiesel A, Miller J, Jolicoeur P, Brisson B. Measurement of ERP latency differences: a comparison of single-participant and jackknife-based scoring methods. Psychophysiology. 2008; 45:250–74. [PubMed: 17995913]

Kristeva-Feige R, Feige B, Makeig S, Ross B, Elbert T. Oscillatory brain activity during a motor task. Neuroreport. 1993; 4:1291–4. [PubMed: 8260607]

Lachaux JP, Rodriguez E, Martinerie J, Varela FJ. Measuring phase synchrony in brain signals. Hum Brain Mapp. 1999; 8:194–208. [PubMed: 10619414]

Lutzenberger W, Preissl H, Birbaumer N, Pulvermuller F. High-frequency cortical responses: do they not exist if they are small? Electroencephalogr Clin Neurophysiol. 1997; 102:64–6. [PubMed: 9060856]

Martinovic J, Gruber T, Muller MM. Coding of visual object features and feature conjunctions in the human brain. PLoS ONE. 2008; 3:e3781. [PubMed: 19023428]

Maunsell JH, Treue S. Feature-based attention in visual cortex. Trends Neurosci. 2006; 29:317–22. [PubMed: 16697058]

McMains SA, Fehd HM, Emmanouil TA, Kastner S. Mechanisms of feature- and space-based attention: response modulation and baseline increases. J Neurophysiol. 2007; 98:2110–21. [PubMed: 17671104]

Miller J, Patterson T, Ulrich R. Jackknife-based method for measuring LRP onset latency differences. Psychophysiology. 1998; 35:99–115. [PubMed: 9499711]

Mirabella G, Bertini G, Samengo I, Kilavik BE, Frilli D, Della Libera C, Chelazzi L. Neurons in area V4 of the macaque translate attended visual features into behaviorally relevant categories. Neuron. 2007; 54:303–18. [PubMed: 17442250]

Müller MM, Keil A. Neuronal synchronization and selective color processing in the human brain. J Cogn Neurosci. 2004; 16:503–22. [PubMed: 15072684]

Nobre AC, Rao A, Chelazzi L. Selective attention to specific features within objects: behavioral and electrophysiological evidence. J Cogn Neurosci. 2006; 18:539–61. [PubMed: 16768359]

Polich J, Kok A. Cognitive and biological determinants of P300: an integrative review. Biol Psychol. 1995; 41:103–46. [PubMed: 8534788]

Roelfsema PR. Cortical algorithms for perceptual grouping. Annu Rev Neurosci. 2006; 29:203–27. [PubMed: 16776584]

Sannita WG, Bandini F, Beelke M, De Carli F, Carozzo S, Gesino D, Mazzella L, Ogliastro C, Narici L. Time dynamics of stimulus- and event-related gamma band activity: contrast-VEPs and the visual P300 in man. Clin Neurophysiol. 2001; 112:2241–9. [PubMed: 11738194]

Schoenfeld MA, Hopf JM, Martinez A, Mai HM, Sattler C, Gasde A, Heinze HJ, Hillyard SA. Spatio-temporal analysis of feature-based attention. Cereb Cortex. 2007; 17:2468–77. [PubMed: 17204821]

Singer W, Engel AK, Kreiter AK, Munk MHJ, Neuenschwander S, Roelfsema PR. Neuronal assemblies: necessity, signature and dectability. Trends in Cognitive Sciences. 1997; 1:252–261. [PubMed: 21223920]

Smid HG, Jakob A, Heinze HJ. An event-related brain potential study of visual selective attention to conjunctions of color and shape. Psychophysiology. 1999; 36:264–79. [PubMed: 10194973]

Tallon C, Bertrand O, Bouchet P, Pernier J. Gamma-range activity evoked by coherent visual stimuli in humans. European Journal of Neuroscience. 1995; 7:1285–1291. [PubMed: 7582101]

Tallon-Baudry C, Bertrand O, Peronnet F, Pernier J. Induced gamma-band activity during the delay of a visual short-term memory task in humans. Journal of Neuroscience. 1998; 18:4244–4254. [PubMed: 9592102]

Tallon-Baudry C, Bertrand O. Oscillatory gamma activity in humans and its role in object representation. Trends in Cognitive Sciences. 1999; 3:151–162. [PubMed: 10322469]

Womelsdorf T, Fries P. Neuronal coherence during selective attentional processing and sensory-motor integration. J Physiol Paris. 2006; 100:182–93. [PubMed: 17317118]

Yuval-Greenberg S, Tomer O, Keren AS, Nelken I, Deouell LY. Transient induced gamma-band response in EEG as a manifestation of miniature saccades. Neuron. 2008; 58:429–41. [PubMed: 18466752]

Zhang W, Luck SJ. Feature-based attention modulates feedforward visual processing. Nat Neurosci. 2009; 12:24–5. [PubMed: 19029890]

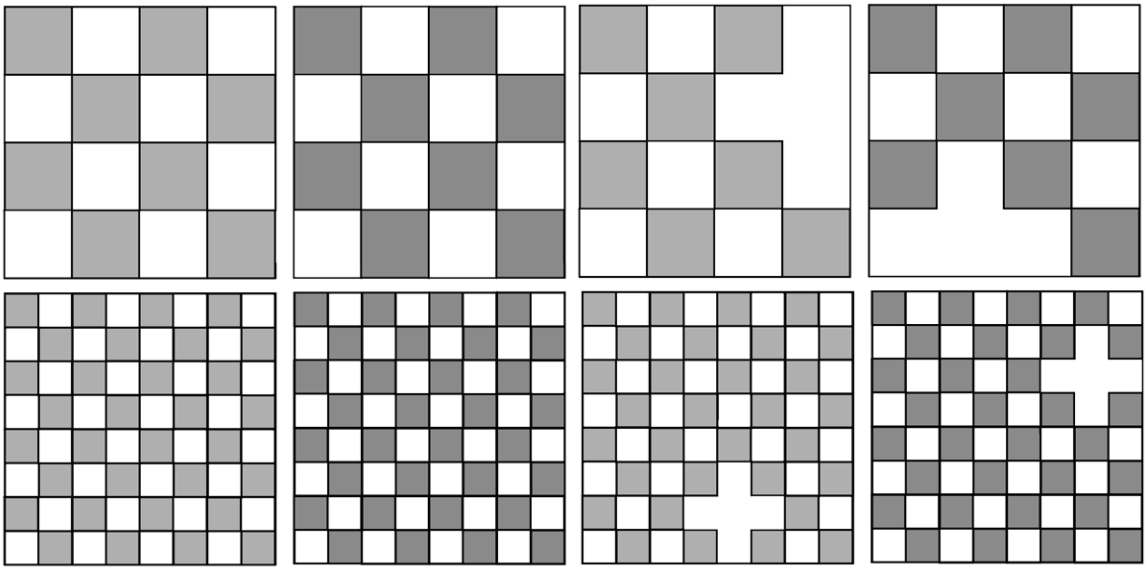

Figure 1.
Grayscale representation of the experimental stimuli used in the present study. In the experiment, stimuli were shown in green or turquoise, differing in terms of one or more of the following stimulus features: color (turquoise, green), check size (large, small), and completeness (complete, one check missing). The completeness feature was always used as the target feature (incomplete checkerboards were always designated to be rare targets) and thus this feature, which was also necessarily confounded with brightness, was not evaluated in the difference waveforms (see methods).

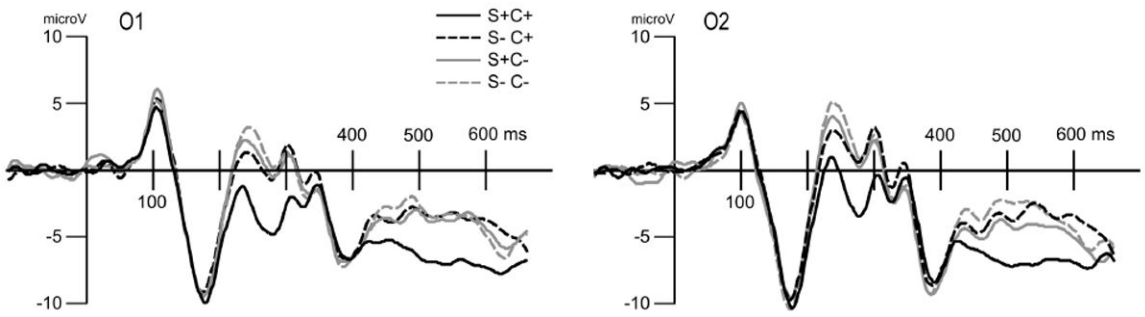

Figure 2.

Grand mean (n=13) ERP waveforms for the four experimental conditions, at two posterior electrode locations (O1 and O2). Positive voltages are up. Parametric sensitivity of the ERP to the number and type of to-be-attended features is visible, beginning at around 200 ms post-stimulus.

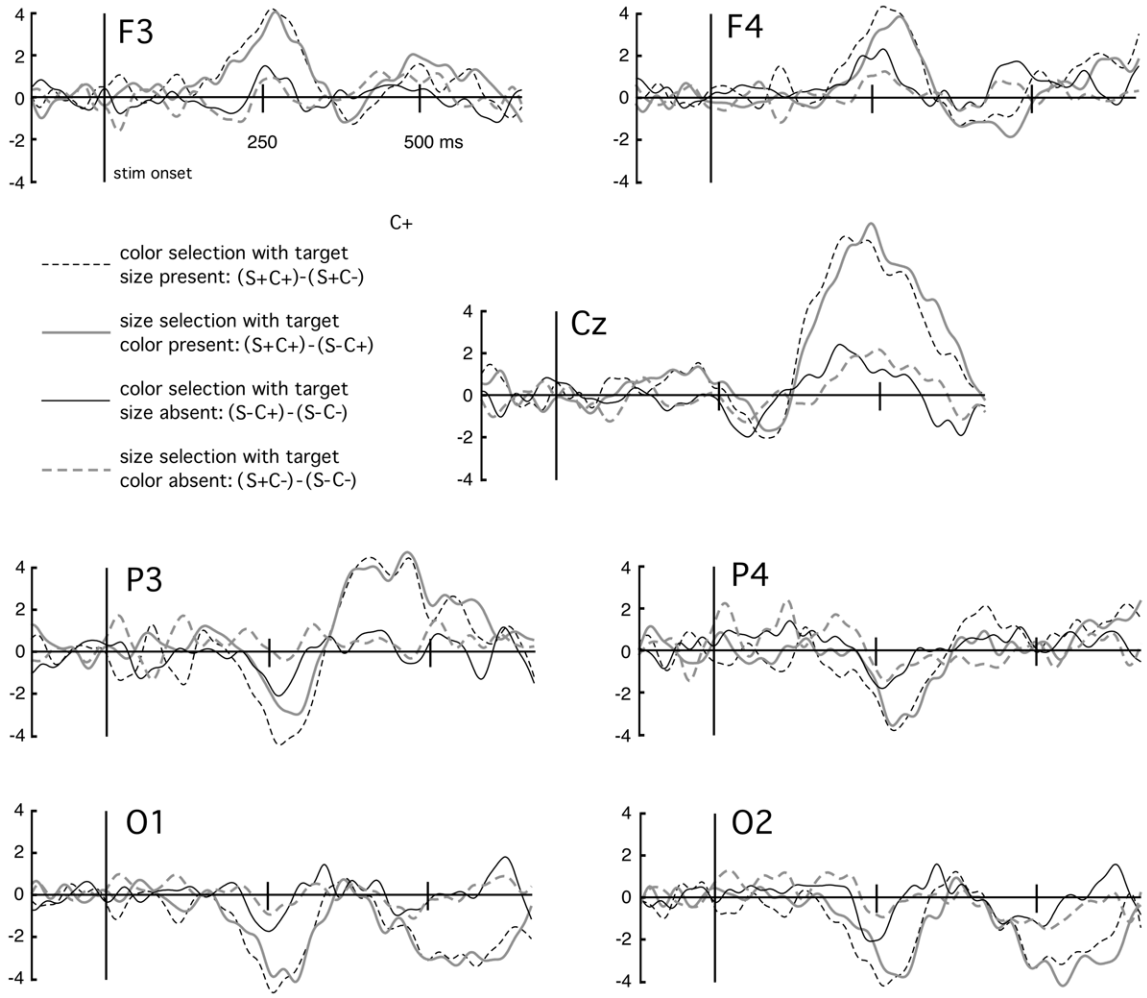

Figure 3.

Grand mean (n=13) ERP differences waveforms for the four condition differences of interest. Seven electrode sites are shown with positive voltages up. Posterior channels show the bi-lateral selection negativity peaking around 250 ms post-stimulus. The negativity is more pronounced when additional target features were present (black dashed, gray solid), compared to when only one target feature was present (gray dashed, black solid). This is consistent with the notion that the selection negativity increases parametrically as more feature-based attention is allocated to a stimulus.

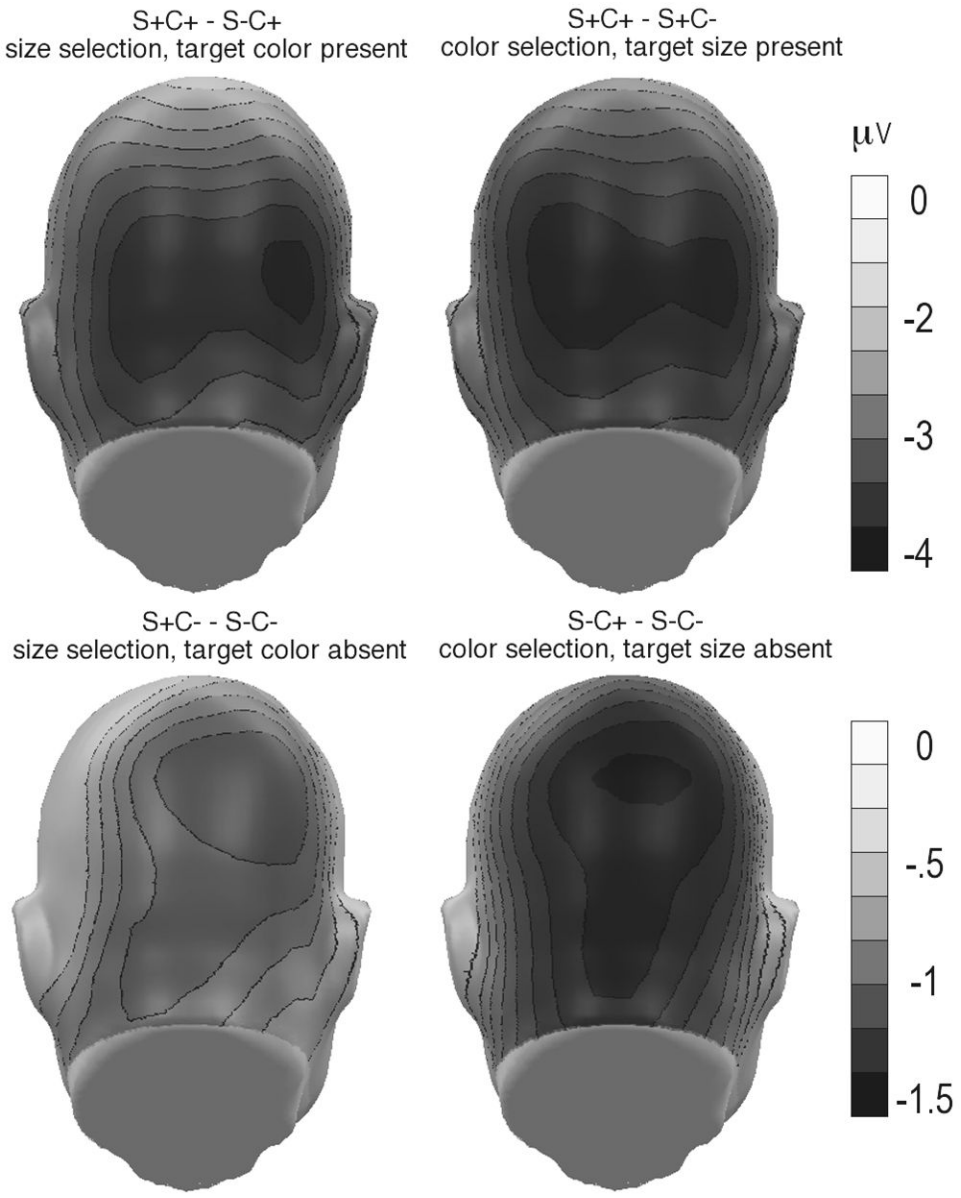

Figure 4.

Grand mean topographical distribution of the selection negativity, averaged across a time range of 180-330 ms post-stimulus, for the four condition differences of interest. A back view is shown. Values reflect a mean across 13 participants. Greater selection negativity across posterior sites is shown for the conditions in which a feature was selected in an object with additional attended features (top) compared to objects with no other attended features (bottom). Note the different scale for the top and bottom rows.

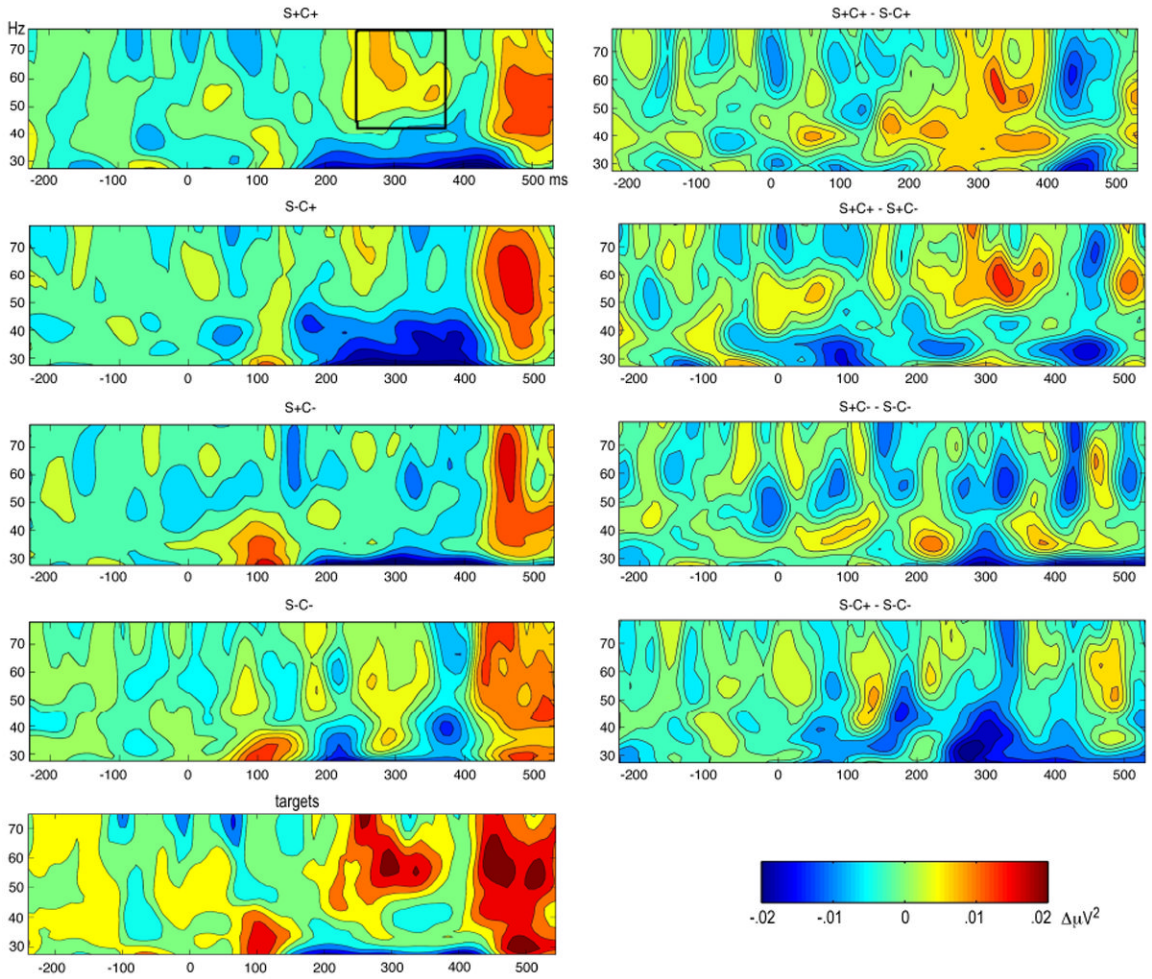

Figure 5.

Grand mean baseline-corrected time by frequency (TF) plots for the four conditions of interest (left) and the four condition differences of interest (right). TF plots on the left show total time-varying energy in the time by frequency plane, including evoked (time and phase-locked) and induced (not time and phase-locked) oscillations. All TF plots contain baseline-corrected time-varying amplitude. The TF plot for the target conditions is shown on the bottom left, for comparison, and was not analyzed in the present study. The top left panel illustrates the TF range of interest, as extracted for statistical analysis (black box). Note that the high-amplitude GBA in the window containing the offset response and the behavioral response decision (i.e. around 500 ms) is similar across the experimental conditions of interest and thus was not related to attention-related differences as shown in the right hand panels.

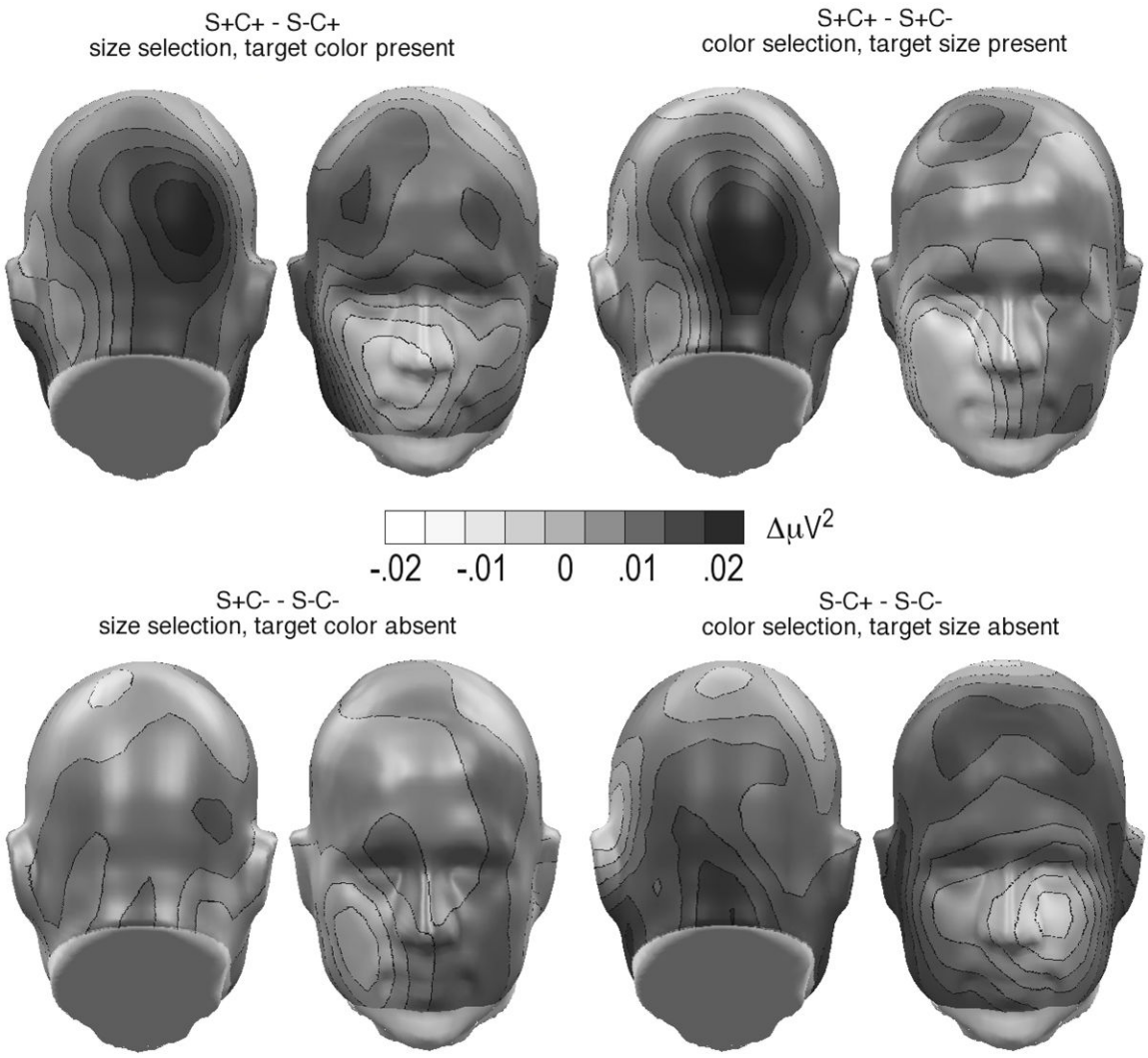

Figure 6.

Spline-interpolated topographical distribution of high induced GBA power changes (back and front views), for the four condition differences of interest. Top row: selection with second target feature present; bottom row: selection with no other target feature present. Note the selective GBA enhancement for stimuli sharing the overall configuration of the target (color and shape). Areas below the nose level in the front view represent extrapolated values.

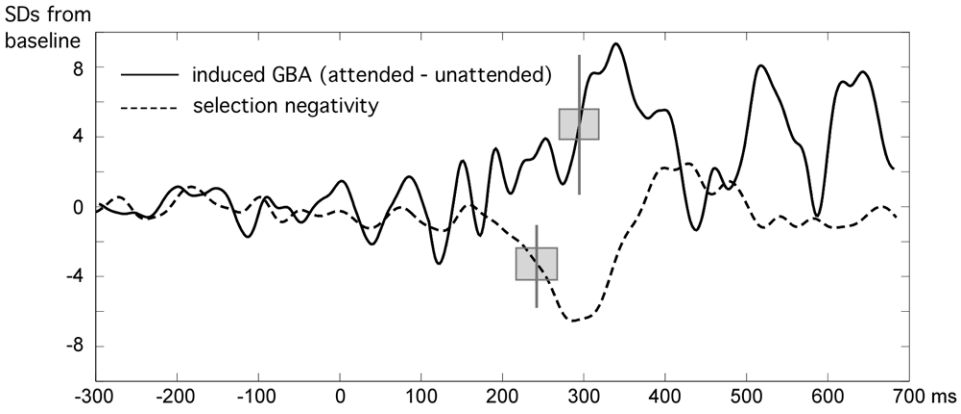

Figure 7.

Grand mean time series for the SN and GBA for the conditions with an additional target feature present (i.e. selection of two features), expressed in standard deviations from a baseline mean. The time series for the GBA was extracted from the posterior sites used for creation of time-frequency plots, i.e., P3/P4, P7/P8, P03/PO4, P07/P08, 01/02, and P9/P10. Thus, the time series mainly reflects late induced GBA, which showed broader topographical distribution. Secondary GBA peaks around 500 and 650 ms reflect non-systematic changes in the response time window (see also the time-frequency plots above). Vertical lines indicate the 50% criterion applied for latency analyses by means of jackknifing; the gray box reflects the jackknifed standard deviation.